Molecular Imaging of Inflammation and Intraplaque Vasa Vasorum

24

Gerrit L. ten Kate, Stijn C.H. van den Oord, Eric J.G. Sijbrands, Antonius F.W. van der Steen, and Arend F.L. Schinkel

Abbreviations

CT	Computed tomography
ED-B	Fibronectin extra-domain B
FDG	^{18}F-Fluorodeoxyglucose
HIF-1α	Hypoxia-inducible factor-1α
ICAM-1	Intercellular adhesion molecule-1
MMP	Matrix metalloproteinase
MRI	Magnetic resonance imaging
PET	Positron emission tomography
SPECT	Single photon emission tomography
SPIO	Super paramagnetic iron oxide
VCAM-1	Vascular cell adhesion molecule-1
VEGF	Vascular endothelial growth factor

G.L. ten Kate (✉) • A.F.L. Schinkel
Division of Pharmacology, Vascular and Metabolic Diseases, Department of Internal Medicine,
Erasmus University Medical Center, Office Ba-304, 's Gravendijkwal 230, 3015 CE, Rotterdam, The Netherlands

Department of Cardiology, Thoraxcenter, Erasmus University Medical Center, Rotterdam, The Netherlands
e-mail: gltenkate@gmail.com; a.schinkel@erasmusmc.nl

S.C.H. van den Oord
Department of Cardiology, Thoraxcenter, Erasmus University Medical Center, Office Ba-304, 's Gravendijkwal 230, 3015 CE, Rotterdam, The Netherlands

Department of Biomedical Engineering, Thoraxcenter, Erasmus University Medical Center, Rotterdam, The Netherlands
e-mail: s.vandenoord@erasmusmc.nl

E.J.G. Sijbrands
Division of Pharmacology, Vascular and Metabolic Diseases, Department of Internal Medicine,
Erasmus University Medical Center, Office D-434, 's Gravendijkwal 230, 3015 CE, Rotterdam, The Netherlands
e-mail: e.sijbrands@erasmusmc.nl

A.F.W. van der Steen
Department of Biomedical Engineering, Thoraxcenter, Erasmus University Medical Center, Office Ee-2302, Gravendijkwal 230, 3015 CE, Rotterdam, The Netherlands
e-mail: a.vandersteen@erasmusmc.nl

1 Introduction

For about half a century invasive angiography has been considered the gold standard in cardiovascular imaging. Angiography provides a high-resolution image of the lumen diameter which makes it able to accurately identify the presence of a lumen narrowing atherosclerotic plaque. In clinical practice the degree of lumen stenosis determined by angiography is frequently the main determinant for the initiation of invasive therapy.

In recent decades it has become apparent that the majority of acute cardiovascular events result from plaques that do not cause a significant stenosis on angiography. A plaque's composition, morphology, and biological processes influence its risk on rupture and thrombosis, which consequently may cause acute cardiovascular events [1–4]. Plaques with properties that make it at risk for rupture and thrombosis have been defined as vulnerable plaques [5]. Two major types of vulnerable plaques have been identified, the rupture prone plaques and the eroded plaques. The rupture prone plaques are thin-cap fibroatheromas, which are characterized by a thin fibrous cap overlying a large necrotic core, containing little smooth muscle cells but numerous macrophages. Eroded plaques have a loss or dysfunction of the luminal endothelium leading to thrombosis, without structural defect to the plaque beyond the endothelium. Eroded plaques are often rich in smooth muscle cells and proteoglycans (Fig. 24.1) [6, 7].

The identification of these vulnerable plaques is expected to improve the prediction of future cardiovascular events. The noninvasive imaging techniques currently available in clinical practice are, besides identifying the degree of lumen stenosis, capable of evaluating plaque size, plaque morphology, and a number of plaque components. However,

L. Saba et al. (eds.), *Multi-Modality Atherosclerosis Imaging and Diagnosis*,
DOI 10.1007/978-1-4614-7425-8_24, © Springer Science+Business Media, LLC 2014

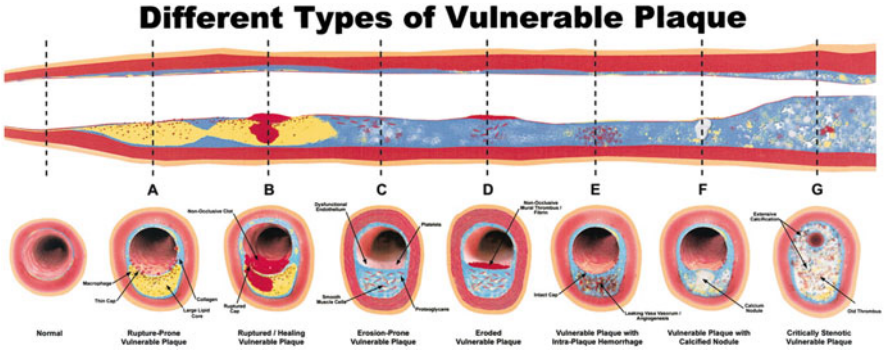

Fig. 24.1 Different types of vulnerable plaque as underlying cause of acute coronary events and sudden cardiac death. (**a**) Rupture-prone plaque with large lipid core and thin fibrous cap infiltrated by macrophages. (**b**) Ruptured plaque with subocclusive thrombus and early organization. (**c**) Erosion-prone plaque with proteoglycan matrix in a smooth muscle cell-rich plaque. (**d**) Eroded plaque with subocclusive thrombus. (**e**) Intraplaque hemorrhage secondary to leaking vasa vasorum. (**f**) Calcific nodule protruding into the vessel lumen. (**g**) Chronically stenotic plaque with severe calcification, old thrombus, and eccentric lumen. Reproduced with permission from Naghavi et al. [5]

especially in the early stages of development the size of most plaque components is too small to accurately image with the current spatial resolution [8, 9]. To date the identification of individual plaque components has not yet resulted in a clinically relevant improvement in prediction [10].

The use of molecular imaging to identify biological processes associated with plaque development and vulnerability could further improve prediction of cardiovascular events. Additionally molecular imaging could detect plaque in an earlier phase of development and provide new insights into the natural history of atherosclerotic disease, and aid the development of new therapies by target selection and validation in vivo, and monitoring of treatment effects [11–13].

The members of the Molecular Imaging Center of Excellence Standard Definitions Task Force have defined molecular imaging as the visualization, characterization, and measurement of biological processes at the molecular and cellular levels in humans or other living systems [14]. Jaffer and Weisleder have formulated four key questions that need to be addressed before molecular imaging can be applied [15].

1. Is there a molecular target relevant to the disease of interest?
2. Once the target is selected, is there a high-affinity ligand that will bind to the target?
3. What is the appropriate molecular imaging modality to provide the required spatial resolution, sensitivity, and depth penetration for the disease?
4. For a given imaging modality, can a molecular imaging agent be synthesized to detect the desired molecular target?

This chapter will review the use of noninvasive molecular imaging for the detection of inflammation and intraplaque neovascularization, two closely related and essential factors in plaque vulnerability. We will focus on the challenges in molecular imaging using nuclear imaging, magnetic resonance imaging (MRI), ultrasound, computed tomography (CT), and multimodality imaging for the evaluation of vulnerable plaques. Implementation of these modalities, for both molecular imaging and molecular guided therapy, will be addressed.

2 Inflammation and Intraplaque Neovascularization

Several molecular targets involved in atherosclerosis have been identified in basic research [16]. Inflammation and neovascularization are of special interest for molecular imaging due to their expression of endothelial markers in the lumen. Many of the molecular contrast agents are relatively large and are therefore restricted to intraluminal targets. The intraluminal expression of molecules associated with neovascularization and inflammation allows for easy targeting. Furthermore, their involvement in the earliest stages of plaque development makes them interesting targets for early detection of plaque development, even before intimal thickening occurs.

The development of an atherosclerotic plaque has long been thought of as a disease originating from the lumen–intima border, initiated by the diffusion of lipids and transportation of monocytes over the luminal endothelium. However, in recent years evidence has been gathered to support the role of the adventitial side of the vessel wall, especially the vasa vasorum, in plaque development [17]. The vasa vasorum form a microvascular network in the vessel wall of large arteries that provides the vessel wall with oxygen and nutrients. The vasa vasorum have been reported to provide an additional endothelial surface area of 17% of the main lumen endothelial surface in normal coronary arteries [18]. This number can rise to about almost 70% in regions with non-calcified plaques [18, 19].

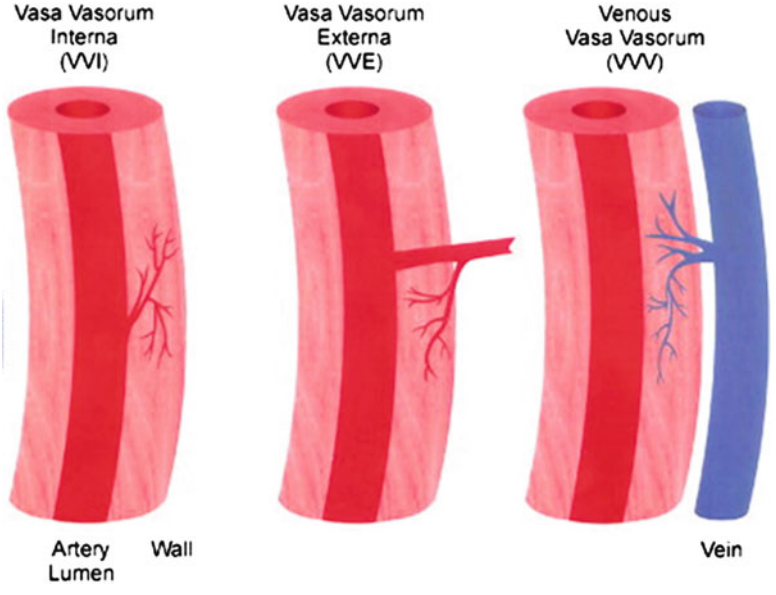

Fig. 24.2 Sketches of the three types of vasa vasorum found in the wall of cow aortae [inspired by Schoenenberger and Mueller 157]. In the Schoenenberger and Mueller study, vasa vasorum interna (*left panel*) originated directly from the aorta's main lumen, and vasa vasorum externa (*mid panel*) originated from intercostal branches deriving from the main lumen and dived back into the aortic wall. Venous vasa vasorum (*right panel*) developed in the aortic wall and finally drained into branches of concomitant veins. Reproduced with permission from Gössl et al. [25]

All cells in the human body are dependent on the vascular system for delivery of oxygen and nutrients. The majority of cells of the arterial vessel wall obtain their oxygen and nutrients by diffusion from the main lumen. However, in vessel walls more than 29 lamellar units thick, diffusion from the lumen is no longer sufficient. In these arteries the delivery to the adventitia and outer media is supplemented by vasa vasorum [20–24].

In humans vasa vasorum are present in all arteries with a vessel wall thickness >0.5 mm [24]. The majority of vasa vasorum originate from side branches of the main artery and enter the arterial wall from the abluminal side (vasa vasorum externa; Fig. 24.2), though vasa vasorum originating directly from the main lumen (vasa vasorum interna) are present as well. Additionally a network of venous vasa vasorum has been identified that drains to veins in proximity to the artery [25]. In a normal vessel the vasa vasorum are restricted to the adventitia and outer parts of the media. However, in atherosclerotic vessels neovascularization sprouting from the vasa vasorum into the intimal parts of the plaque has been found [26, 27]

Intraplaque neovascularization has gained interest as a factor in the development, progression, and vulnerability of atherosclerotic plaques. Pathologic studies have shown that the presence of intraplaque neovascularization, especially in the plaque shoulder where the plaque is most vulnerable to rupture, is associated with vulnerable and symptomatic plaques [18, 26–28]. Additionally, the presence of intraplaque neovascularization has been found to be an independent predictor of intraplaque hemorrhage and plaque rupture [27, 29]. Hellings et al. [30] investigated whether plaque composition is associated with the occurrence of future cardiovascular events. Endarterectomy specimens were collected for histology and patients were followed for 3 years after endarterectomy. Patients with intraplaque neovascularization or intraplaque hemorrhage were found to be at increased risk for a combined endpoint of cardiovascular events (fatal or nonfatal stroke, fatal or nonfatal myocardial infarction, sudden death or other vascular death) and any arterial vascular intervention not planned at time of inclusion (Fig. 24.3). The presence of macrophages, a large lipid core, calcifications, collagen, or smooth muscle cells was not associated with clinical outcome [30].

The association between intraplaque neovascularization, intraplaque hemorrhage, and cardiovascular events is thought to be due to the poor structural integrity of the newly formed vasa vasorum [31]. The majority of neovessels in symptomatic plaques are highly irregular in shape, while very few of these irregular vessels are present in asymptomatic plaques [32]. The newly formed microvessels are thin-walled, with incomplete or absent endothelial gap junctions. This may result in the extravasation of lipids, inflammatory cells, and red blood cells, and risks the collapse of microvessels, causing intraplaque hemorrhage (Fig. 24.4). This will contribute to lipid core growth and sustained plaque inflammation, thus the progression into more advanced plaques [33, 34]. Consequently plaques with a high density of neovascularization are at an increased risk of plaque rupture [35, 36].

Angiogenesis, the sprouting of new microvessels from an existing microvascular network, is the main process resulting in neovascularization of atherosclerotic plaques [35, 37]. Key factors initiating angiogenesis in atherosclerosis are still largely unknown. Developments in tumor research have greatly increased our knowledge about the processes that take place during neovascularization and identified several factors that can initiate neovascularization such as metabolic stress (hypoxia, acidosis, or hypoglycaemia),

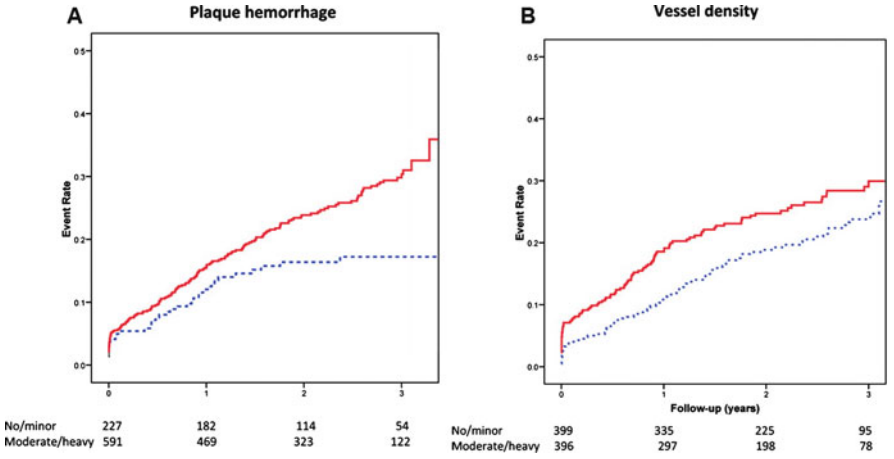

Fig. 24.3 Kaplan–Meier survival curves of plaque histology vs. primary outcome (vascular event and vascular intervention) for plaque hemorrhage (**a**): absent (*dashed line*) vs. present (*continuous line*) and intraplaque vessel density (**b**): <8 (average number of vessels per hot spot, dashed line) vs. ≥8 vessels (*continuous line*). The number of patients at risk for systemic cardiovascular events at 0, 1, 2, and 3 years is provided. Reproduced with permission from Hellings et al. [30]

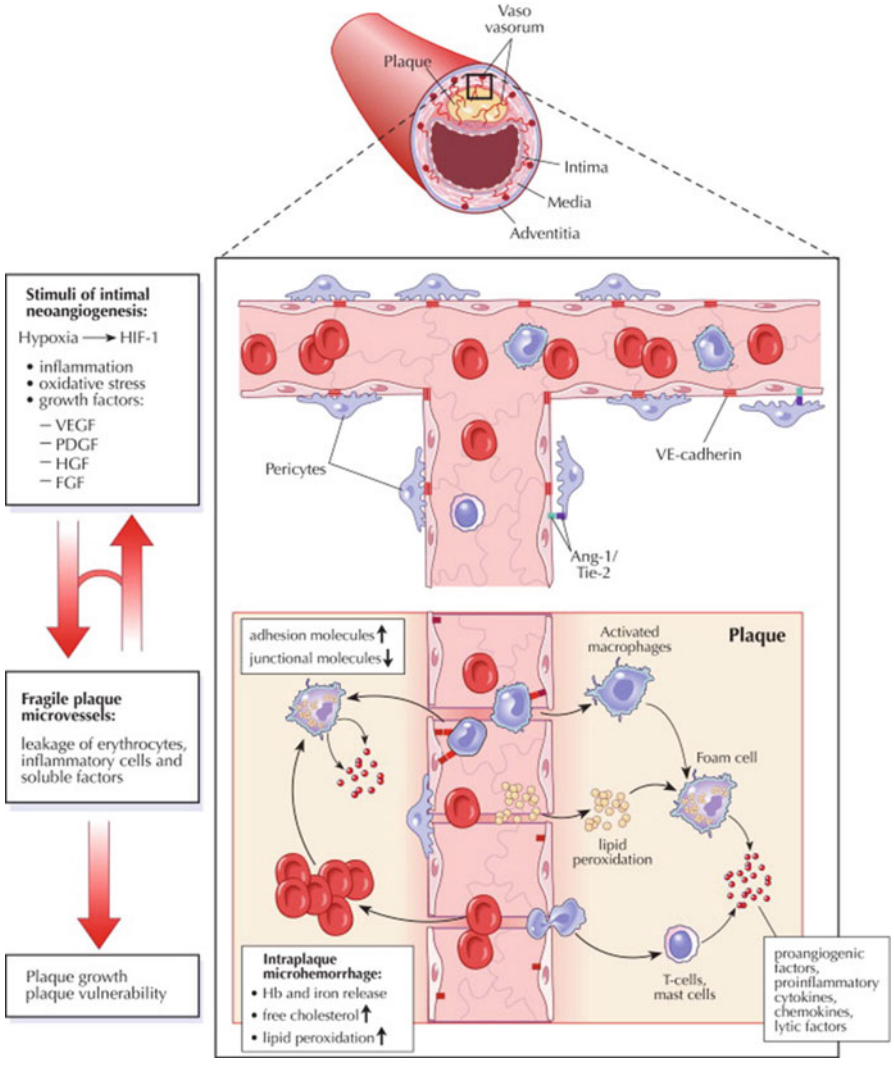

Fig. 24.4 Plaque microvessels show a compromised structural integrity and a modified expression profile of adhesion and junctional molecules, thus permitting extravasation of inflammatory cells and soluble factors as well as the occurrence of microhemorrhages. The resulting reactive microenvironment may support further plaque growth and plaque vulnerability. *Ang* angiopoietin, *FGF* fibroblast growth factor, *Hb* hemoglobin, *HGF* hepatocyte growth factor, *HIF* hypoxia-inducible factor, *PDGF* platelet-derived growth factor, *VE* vascular endothelial, *VEGF* vascular endothelial growth factor. Figure illustration by Rob Flewell. Reproduced with permission from Mause and Weber [31]

mechanical stress (pressure generated by proliferating cells), immune/inflammatory response (immune/inflammatory cells that have infiltrated the tissue), and genetic mutations [38].

Hypoxia has been found to be one of the most important stimuli for angiogenesis in several diseases [39, 40]. Upregulation of hypoxia-inducible factors has been found in

Table 24.1 Brief comparison of technological features of noninvasive imaging modalities used in clinical practice

Imaging modality	Spatial resolution (mm)	Acquisition time/frame (s)	Sensitivity of detection (g/ml)	Anatomical detail	Plaque composition	Advantages	Disadvantages
PET	3–8	1–300	$<10^{-12}$	−	−	Quantitative measurements	Ionizing radiation
							Short half-life tracers
							Expensive equipment
							Requires on-site cyclotron
SPECT	5–12	60–2,000	$>10^{-9}$	−	−	Multiple isotope imaging	Ionizing radiation
MRI	0.1–0.2	50–3,000	$>10^{-6}$	++	+++	No ionizing radiation	Contrast-induced systemic fibrosis
						Widely available	
Ultrasound	0.1–1.0	0.05–1	NA	+	+	No ionizing radiation	Limited penetration depth
						Widely available	Obligatory intravascular contrast agent
						Inexpensive	
						Real-time imaging	
CT	0.5–1	1–300	$>10^{-3}$	+++	+	Coronary imaging	Ionizing radiation
						Widely available	Contrast nephrotoxicity

CT computed tomography, *MRI* magnetic resonance imaging, *NA* not available, *PET* positron emission tomography, *SPECT* single photon emission computed tomography. Table based on ten Kate et al. [154]

atherosclerotic plaques [41, 42]. Though hypoxia may arise due to the increasing distance between the vessel lumen and plaque core, this is unlikely to be the main culprit, since angiogenesis is already present in early stages of plaque development when intimal thickening is negligible [43–46]. Hypoxia is thought to be primarily determined by the increased oxygen demand caused by plaque inflammation [35].

Inflammation is one of the hallmarks of plaque development and vulnerability and inflammatory cells have generally been accepted to play a key role in the early stages of plaque formation. In the early stages the vessel wall is infiltrated by lipoproteins and as a response the endothelium expresses leukocyte adhesion molecules. Monocytes in the lumen adhere to the adhesion molecules and extravasate into the subintimal space [47]. The influx of monocytes and their subsequent differentiation into mature and activated inflammatory cells increases the metabolic demand in the vessel wall. If the supporting vasculature is insufficient this will result in a hypoxic state and increased oxidative stress. This hypothesis has been supported by the presence of both hypoxic and inflammatory factors, such as hypoxia-inducible factor-1α (HIF-1α), nuclear transcription factor-kappa B, tumor necrosis factor-α, and interleukin-6 and an increased number of superoxide anions in atherosclerotic plaques. Furthermore, these factors have been found to be co-localized with intraplaque neovascularization [41, 48, 49].

3 Imaging Modalities

The noninvasive imaging modalities currently utilized in clinical practice are after the administration of a specialized contrast agent (e.g., iron oxide, gadolinium, microbubbles, radionuclides, iodine, gold, bismuth) capable of molecular imaging (Table 24.1).

Nuclear Imaging Nuclear imaging includes a number of techniques that are all dependent on a physical signal emitted by a radionuclide tracer. The two predominant techniques currently in use are positron emission tomography (PET) and single photon emission computed tomography (SPECT). Both techniques have a high penetration depth and are capable of 3D whole body scanning.

Inherent to the dependency on a physical signal is the very high sensitivity with which nuclear imaging can detect the molecular tracer [50]. The main drawbacks of nuclear imaging are the limited spatial resolution, and the lack of anatomical information. This is partially overcome by co-registration with either CT or MRI to provide high-resolution anatomical information. The use of radionuclide tracers has the inherent problem of radiation exposure of both personnel and patient. Though the radiation doses currently used in clinical practice are safe, the effect of cumulative radiation

exposure should be taken into account when performing repeated measurements.

Magnetic Resonance Imaging MRI molecular imaging is performed using either gadolinium or superparamagnetic iron oxide compounds (SPIOs) that influence the magnetic resonance signal. MRI provides a sub-millimeter spatial resolution and good soft tissue contrast, thus providing an excellent evaluation of anatomical structures. In recent years increasing field strengths and improved coil designs have resulted in higher signal-to-noise ratios, contrast-to-noise ratios, and resolutions, while reducing scanning times. Additionally MRI can obtain anatomic, physiologic, and metabolic information in one session.

The primary disadvantage is the low sensitivity for the detection of the contrast agent compared to nuclear techniques [51]. Additionally the use of gadolinium has been associated with nephrogenic systemic fibrosis, especially in patients with reduced renal function [52].

Ultrasound B-mode and Doppler ultrasound are the most frequently utilized imaging modalities in clinical practice. Ultrasound has a high spatial resolution, which provided excellent anatomical information. Ultrasound contrast agents consist of gas-filled microbubbles stabilized by a lipid or protein shell. For molecular imaging ligands can be bound to these microbubbles. When using specific pulse sequences ultrasound is capable of specific contrast imaging, which eliminates the signal of the surrounding tissue. This makes ultrasound very sensitive for the detection of contrast agent [53]. Untargeted ultrasound contrast agents have been used in echocardiography for decades and have been proven safe in large multicenter studies [54, 55].

Ultrasound has a superior temporal resolution, which makes it the only technique currently available for real-time imaging. However, the penetration depth and 3D scanning capabilities are limited. Another important limitation is the relatively large size (1–5 μm) of the microbubbles, making them obligatory intravascular tracers. However, this makes them well suited for identifying the presence of vasculature, since the presence of contrast agent indicates the presence of a vessel.

Computed Tomography CT (especially the latest generations of multislice and dual source CT) provides a high-resolution image with very short acquisition times, good penetration depth, and full body scanning capabilities. CT is currently the only noninvasive technique in clinical practice with sufficient resolution, penetration, and speed to accurately image the coronary arteries in a beating heart. CT provides good anatomical information; however, it is poor in soft tissue contrast. However, the use of CT for molecular imaging of the coronary arteries has not yet been investigated.

Molecular CT contrast agents are in early stage of development. Molecular contrast agents based on iodine, gold, and bismuth have been developed; however, they have not yet been investigated in humans [56–59]. The use of ionizing radiation potentially limits the use of CT, though the radiation dose in cardiovascular imaging has substantially been reduced in recent years [60]. From clinical practice it is known that iodine contrast agents can induce a contrast nephropathy, limiting its use in patients with decreased renal function [61].

Multimodality Imaging is being explored to improve the accuracy of examinations. The currently available modalities each have their limitations as previously described. When using multiple imaging modalities the advantages of each individual modality can be used to the other modalities' limitations, in order to improve the overall accuracy. In clinical practice multimodality imaging is already used by combining nuclear imaging with co-registration of either CT or MRI. This allows for the combination of the highly accurate and quantifiable assessment of biological activity by nuclear imaging with the high-resolution anatomical information provided by CT or MRI (Fig. 24.5) [62, 63].

The use of multimodal contrast agents is currently limited to preclinical research. A number of probes have been developed that enable both in vivo and ex vivo molecular imaging (e.g., MRI and fluorescence [64]). However, probes that are detectable with multiple in vivo imaging modalities (e.g., MRI and PET [65]) are sparse. The development of multimodal probes could help achieve high sensitivity and high spatial resolution.

4 Molecular Targets

Leukocyte Adhesion Molecules The expression of leukocyte adhesion molecules is a marker of endothelial dysfunction and is pivotal in the initiation of vessel wall inflammation [47]. Since adhesion molecules are expressed in the vascular lumen they are easily accessible to molecular contrast agents. Frequently investigated adhesion molecules include vascular cell adhesion molecule-1 (VCAM-1), intercellular adhesion molecule-1 (ICAM-1), and selectins. VCAM-1 and ICAM-1 and selectins are expressed by the luminal endothelium overlying the atherosclerotic plaque. However, the most dominant expression has been found at the adventitial site of the plaque and correlated with sites of vasa vasorum neovascularization, vascular permeability, and a high number of inflammatory cells [66, 67].

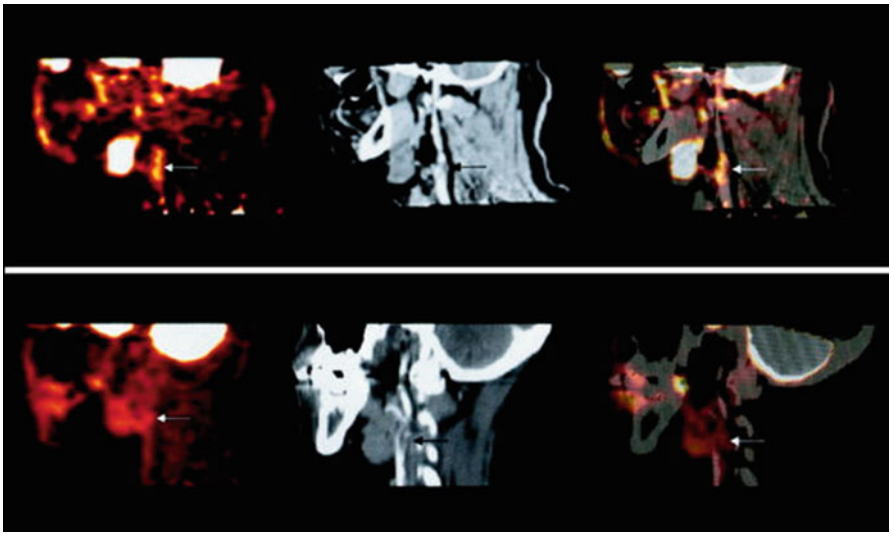

Fig. 24.5 The *upper row* (from *left* to *right*) shows PET, contrast CT, and co-registered PET/CT images in the sagittal plane, from a 63-year-old man who had experienced two episodes of left-sided hemiparesis. Angiography demonstrated stenosis of the proximal right internal carotid artery; this was confirmed on the CT image (*black arrow*). The *white arrows* show FDG uptake at the level of the plaque in the carotid artery. As expected, there was high FDG uptake in the brain, jaw muscles, and facial soft tissues. The *lower row* (from *left* to *right*) demonstrates a low level of FDG uptake in an asymptomatic carotid stenosis. The *black arrow* highlights the stenosis on the CT angiogram, and the *white arrows* demonstrate minimal FDG accumulation at this site on the FDG-PET and co-registered PET/CT images. Reproduced with permission from Ross et al. [93]

VCAM-1-targeted MRI contrast agents have utilized VCAM-1's ability to internalize ligands, resulting in accumulation of the contrast agent. In vivo VCAM-1-targeted magnetofluorescent nanoparticles were shown to be able to identify VCAM-1 expression in atherosclerotic lesions by MRI, which was confirmed by fluorescence imaging and histology [68, 69]. In ex vivo endarterectomy specimens it was confirmed that the VCAM-1-targeted contrast agents co-localized with VCAM-1 expressing endothelial cells in human plaques as well [69]. Additionally it was shown that statin therapy reduced the contrast enhancement caused by the VCAM-1-targeted contrast on MRI and fluorescence imaging (Fig. 24.6), which correlated with reduced expression of VCAM-1 on histology [69]. (Table 24.2).

A VCAM-1-targeted contrast agent has also been developed for ultrasound [70]. In vitro experiments showed that VCAM-1-targeted microbubbles were able to attach to activated murine endothelial cells, even under a pulsatile high shear stress condition. Subsequent in vivo experiments showed ultrasound signal enhancement in the aortic plaques of apoE-deficient mice within 10 min after contrast injection [70]. These results suggest that VCAM-1-targeted microbubbles could provide a fast molecular imaging technique. The availability of a fast molecular imaging technique could be advantageous for clinical practice.

Similarly, ICAM-1-targeted microbubbles were shown to specifically bind to endothelial cells expressing ICAM-1 in vitro [71]. In vivo ICAM-1-targeted microbubbles were found to attach to what are described as early stages of the atherosclerotic plaque (Fig. 24.7) [72]. Though this study showed that ultrasound might be capable of identifying the early stages of atherosclerotic vascular disease, no histology was performed to confirm this finding.

Selectin-targeted contrast agents have been developed but not yet investigated for the imaging of atherosclerotic plaques. Both e-selectin- and p-selectin-targeted SPIO compounds have shown binding to human endothelial cells in vitro and a concomitant significant T2 signal decrease on MRI [73–75]. e-Selectin-targeted MRI contrast agents have been used in vivo to identify inflammation in hepatic and muscle tissue of mice [76, 77].

Inflammatory Cells The activated endothelium releases chemoattractants to recruit monocytes. These subsequently enter into the sub-endothelial space where they differentiate in mature inflammatory cells. Macrophages are the most prevalent inflammatory cell in the atherosclerotic plaque and play a major role in the pathophysiology of plaque vulnerability [78]. The macrophages can cause a maladapted chronic inflammatory response that will aid the expansion of the sub-endothelial layer due to the accumulation of cells, lipids, and matrixmolecules [78]. The presence of macrophages in the plaque has been found to be closely associated with intraplaque neovascularization [79]. Macrophages both use the vasa vasorum neovascularization

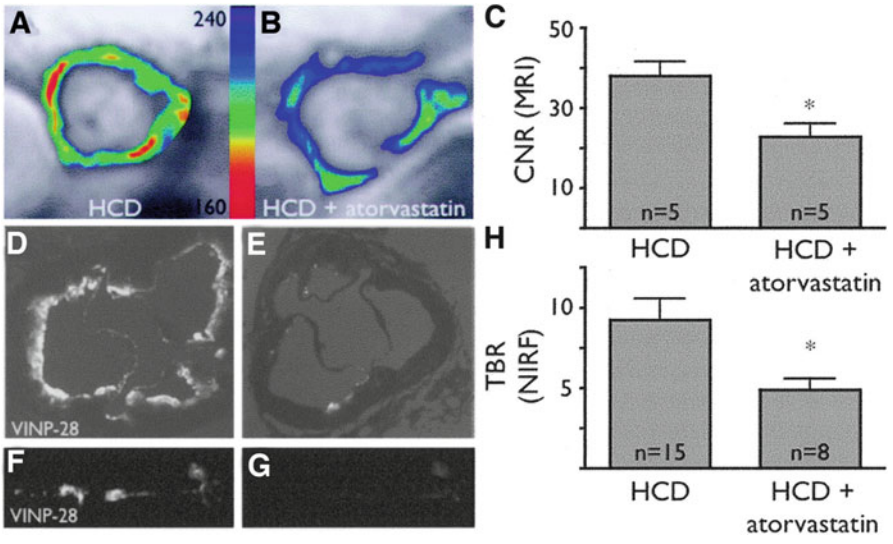

Fig. 24.6 Noninvasive MRI assessment of VCAM-1 expression after atorvastatin administration. (**a**) Short-axis MRI of the aortic root of an untreated apoE$^{-/-}$ mouse on a high cholesterol diet (HCD) after injection of a VCAM-1-targeted nanoparticle (VINP-28) with color-coded signal intensity. The *red color* encodes high VCAM-1 expression. (**b**) MRI of HCD + atorvastatin-treated apoE$^{-/-}$ mouse after VINP-28 injection. An attenuated signal drop in the aortic root wall compared with untreated mouse was noted. (**c**) After injection of VINP-28, the MRI contrast-to-noise ratio diminished in atorvastatin-treated mice (mean ± SD; $^*P < 0.05$ versus HCD). (**d**, **e**) Near-infrared (NIR) microscopy of the aortic roots depicted in **a** and **b**. Fluorescent signal originating from VINP-28 comprised the whole-root circumference (**d**), but less so in atorvastatin-treated mice (**e**). (**f**, **g**) Fluorescent reflectance imaging of the excised aorta of an untreated (**f**) and atorvastatin-treated (**g**) mouse showed reduced NIR signal in statin-treated mice. (**h**) The target-to-background ratio was reduced in aortas of treated mice (mean ± SD;$^*P < 0.05$ treated vs. untreated mice). Reproduced with permission from Nahrendorf et al. [69]

Table 24.2 Available studies on potential molecular targets involved in neovascularization and inflammation of the atherosclerotic plaque

Target	Nuclear imaging	MRI	Ultrasound	CT	In vivo imaging	Atherosclerosis model
Leukocyte adhesion molecules						
VCAM-1		[68, 69, 75]	[70, 132]		Animal	Yes
ICAM-1		[155]	[71, 72, 133]		Animal	Yes
e-Selectin		[73, 74, 76, 77]	[133]		Animal	No
p-Selectin		[75]	[132, 134]		No	Yes
Inflammatory cells						
Phagocytosis		[80–87]		[56]	Animal	Yes
Macrophage metabolism	[88–100]				Animal	Yes
					Human	Yes
MMP	[103]	[102]			Animal	Yes
Myeloperoxidase		[104]			Animal	Yes
Angiogenesis						
VEGFR2			[113–115, 134]		Animal	No
Endoglin	[112]		[113]		Animal	No
Integrin αvβ3	[122–125]	[120, 121]	[114, 126, 127, 134]		Animal	Yes
					Human	No
Fibronectin ED-B	[130, 131]				Animal	No
					Human	No

CT computed tomography, *ED-B* extra-domain B, *MRI* magnetic resonance imaging, *VEGFR2* vascular endothelial growth factor receptor 2, *ICAM-1* intercellular adhesion molecule-1, *MMP* matrix metalloproteinase, *MRI* magnetic resonance imaging, *VCAM-1* vascular cell adhesion molecule-1

as a port of entry into the plaque and excrete a myriad of proangiogenic molecules aiding the expansion of the microvascular network.

Macrophages provide a number of attractive targets for molecular imaging. Their ability to phagocytose molecules can be utilized to accumulated contrast agent. This should improve the target-to-background ratio and thus the accuracy with which contrast agent can be detected. Activated macrophages have been shown to internalize and concentrate a number of nanoparticles. For example, in

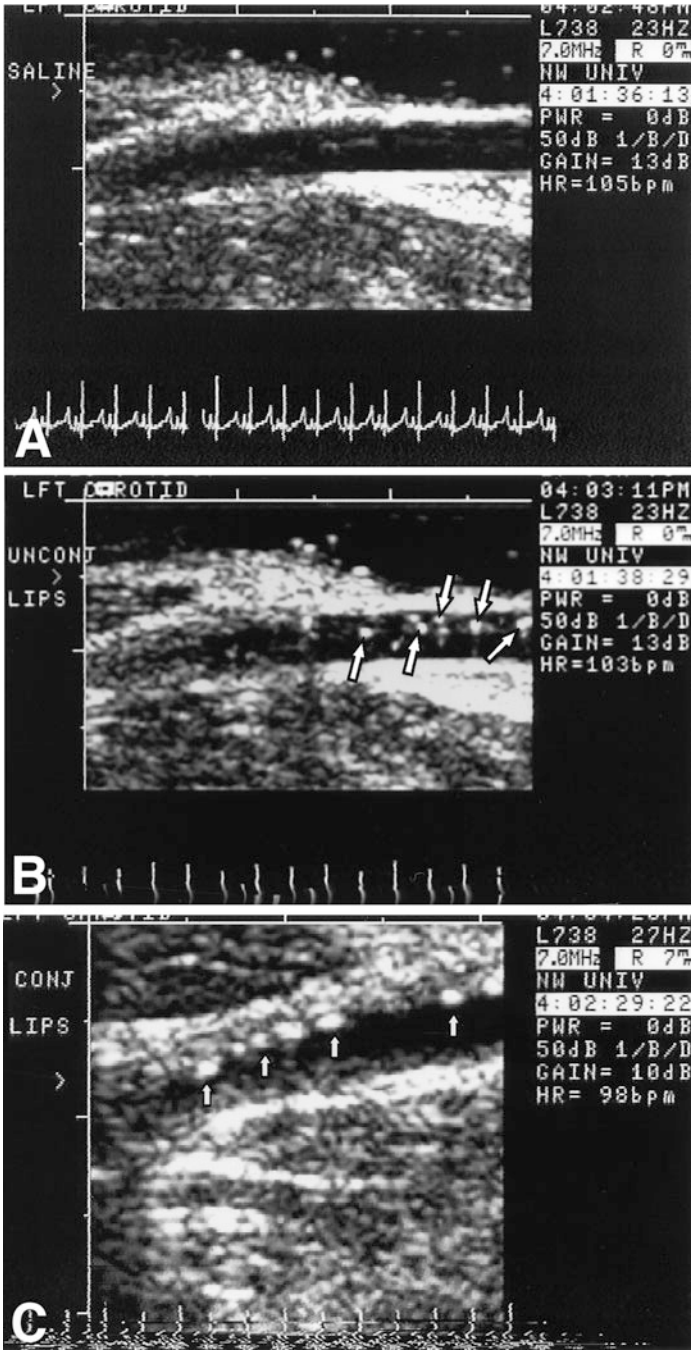

Fig. 24.7 Transvascular ultrasound images of an atherosclerotic left carotid artery of a Yucatan miniswine. (**a**) After injection of saline. (**b**) After injection of unconjugated liposomes (*arrows* point to liposomes within the lumen). (**c**) After injection of anti-ICAM-1-labeled liposomes (*arrows* point to liposomes attached to the atherosclerotic plaque). Reproduced with permission from Demos et al. [72]

vitro macrophages have been shown to actively phagocytose dextran-coated SPIO nanoparticles under the influence of cytokines, serum components, and statin treatment [80]. Similarly, both gadolinium micelles and iodinated nanoparticles have been shown to be internalized by macrophages [56, 81].

Dextran-coated SPIO nanoparticles have been investigated in human endarterectomy patients. The SPIO nanoparticles were shown to be to be able to identify macrophages in vivo [82–86]. However, due to the long interval between pre- and post-contrast scans (≥24 h) the clinical application of SPIO nanoparticles seems limited.

The Atorvastatin Therapy: Effects on Reduction of Macrophage Activity (ATHEROMA) Study investigated the effects of low-dose (10 mg) and high-dose (80 mg) atorvastatin on carotid plaque inflammation as determined by ultrasmall SPIO compound. The primary endpoint was the change in signal intensity from baseline after 6 and 12 weeks of either low-dose or high-dose atorvastatin. Both at 6 and 12 weeks there was a significant reduction in signal intensity from baseline in the high-dose group (Fig. 24.8). There was no difference observed in the low-dose group [87].

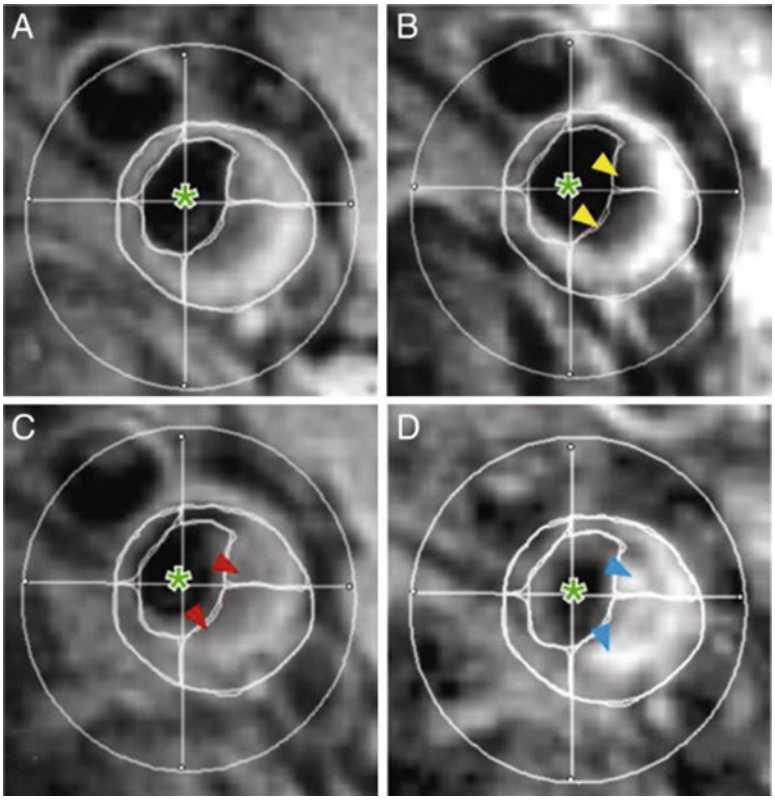

Fig. 24.8 T2*-weighted MRI images of the right common carotid artery of a patient receiving 12 weeks of high-dose atorvastatin (80 mg) treatment. Imager were taken before (*left*) and after (*right*) ultrasmall superparamagnetic iron oxide (USPIO) infusion at time points 0 (**a** and **b**) and 12 weeks (**c** and **d**). (**b**) USPIO uptake can clearly be seen in the plaque at baseline (*yellow arrowheads*). (**c**) USPIO has been cycled out of the plaque before reinfusion at 12 weeks (*red arrowheads*). (**d**) The plaque enhances at 12 weeks (*blue arrowheads*), indicating that the high-dose statin treatment has damped the USPIO-defined inflammation. Plaque segmentation was performed using a combination of multicontrast sequences. The cross hairs centered through the middle of the lumen divide the vessel into quadrants. Signal from artifact, extravascular structures, and the luminal blood pool (*green asterisks*) are excluded from the analysis. Reproduced with permission from Tang et al. [87]

To further improve the accumulation of contrast agent molecular contrast agents have been targeted at the macrophage scavenger receptors, to induce uptake of the molecule. In an in vivo study Lipinski et al. showed that the uptake of gadolinium immuno-micelles targeted at the macrophage scavenger receptor was significantly higher than nontargeted micelles. These promising results suggest that scavenger receptor-targeted contrast agents may improve the detection of macrophages [81].

A second characteristic that can be identified is the high metabolic activity of activated macrophages. The presence of activated macrophages in the atherosclerotic plaque will increase the metabolic activity at that location. The increased metabolic activity can be visualized by ^{18}F-fluorodeoxyglucose (FDG) PET, a radionuclide-labeled glucose analogue taken up by cells in proportion to their metabolism, especially glycolysis. FDG-PET is readily used in clinical practice to identify the presence of malignant metastasis. In cancer patients it was observed that the presence of FDG uptake in the arterial wall was associated with the presence of atherosclerotic vascular disease [88] Subsequently, the in vivo visualization and quantification of plaque inflammation by FDG-PET has been validated against histology in animals [89–92] and humans [93–97].

The use of FDG-PET has been shown to identify possible culprit lesions that were not identified by angiography. Davies et al. [98] investigated 12 patients who had all suffered a recent transient ischemic attack. Ten patients had a high FDG uptake in a plaque in the vascular territory compatible with the symptoms. Three of those were non-stenotic plaques which were not identified as the culprit lesion on angiography. This study shows the possibility of FDG-PET to identify relevant carotid lesions beyond stenosis. However, no histology was obtained to confirm the findings [98].

Rominger et al. [99] followed a cohort of 334 cancer patients asymptomatic for cardiovascular disease who had undergone FDG-PET/CT. Maximal standard uptake values were measured and calcifications were recorded for in both common carotid arteries, ascending aorta, aortic arch, descending aorta, abdominal aorta, and both iliac arteries.

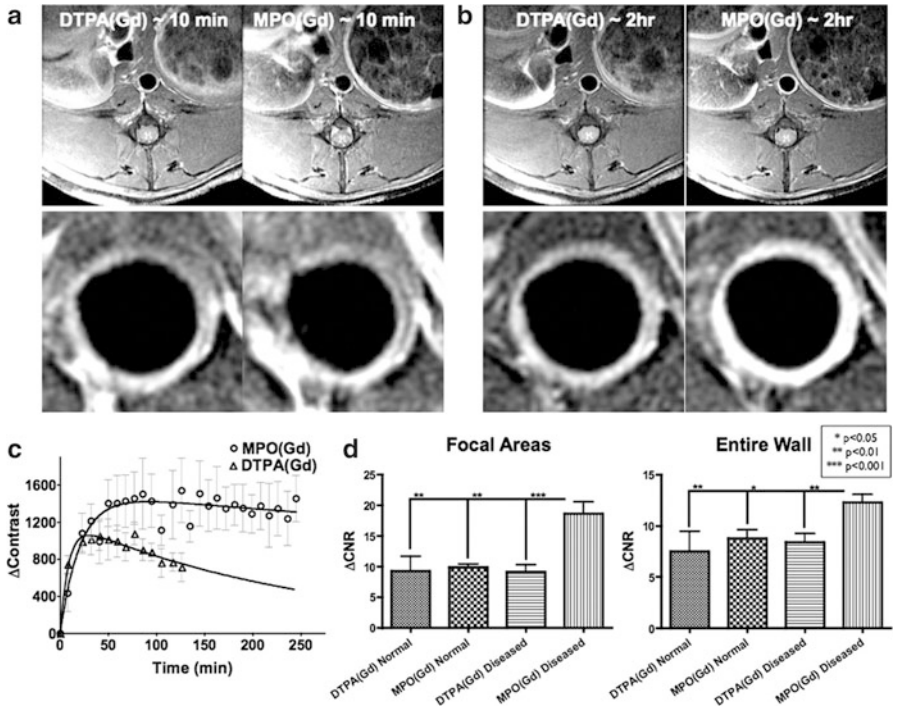

Fig. 24.9 (**a**) As-acquired (*top*; 5-cm field-of-view) and higher magnification (*bottom*; centered around aorta) early-phase (≈10 min) MRI images of diseased wall in rabbit fed a cholesterol diet for 17 months, taken after administration of a gadolinium contrast agent (DTPA(Gd)) (*left*) and a functional myeloperoxidase activity imaging sensor (MPO(Gd)) (*right*). Similar levels of enhancement were seen at this time point with both agents. (**b**) Delayed MPO(Gd) images (≈2 h; *right*) showed substantially increased enhancement compared with both late-phase (≈2 h; *left*) and early-phase (seen in **a**) DTPA(Gd) images. (**c**) Kinetics study. Increased and prolonged contrast was found with MPO(Gd) compared with DTPA(Gd) ($n = 3$ animals). (**d**) Analysis of pre-contrast and 2-h post-contrast [MPO(Gd) and DTPA(Gd)] MR images of rabbits fed a cholesterol diet for 28–29 months ($n = 8$) and age-matched controls ($n = 4$). Δ contrast-to-noise ratio (CNR) in both focal wall areas (*left*) and the entire wall (*right*) revealed no difference from MPO(Gd) and DTPA(Gd) in normal wall ($n = 4$, 11 sections analyzed). Diseased wall imaged with DTPA(Gd) ($n = 8$, 24 sections analyzed) also showed no difference compared with normal wall imaged with either agent. In distinction, diseased wall imaged with MPO(Gd) ($n = 8$, 24 sections analyzed) showed significantly higher ΔCNR (≈2×) than all other values. Reproduced with permission from Ronald et al. [104]

Fifteen patients developed a cardiovascular event in a median follow-up of 29 months. The mean target-to-background ratio (hazard ratio, 14.144; $p = 0.001$) and calcified plaque sum (hazard ratio, 3.560; $p = 0.025$) were significant independent predictors for the occurrence of cardio- or cerebrovascular events [99]. Additionally Tahara et al. [100] have shown the potential of FDG-PET to evaluate the effect of statin treatment on plaque inflammation. After 3 months of statin treatment FDG uptake in the atherosclerotic plaque was significantly decreased, compared to dietary management only [100].

Macrophages also secrete numerous pro-angiogenic factors that are associated with plaque vulnerability, such as matrix metalloproteinases (MMPs). MMPs are a group of enzymes that aid in angiogenesis by degrading the ECM. ECM degradation is necessary to allow for the migration of endothelial cells across the basement membrane. Besides aiding in angiogenesis MMPs have a direct effect on plaque vulnerability by weakening the fibrotic cap overlying the lipid necrotic core [101]. MMP-targeted tracers have been developed for MRI and SPECT [102, 103]. Ohshima et al. investigated a ^{99m}Tc-labeled broad spectrum MMP inhibitor to identify MMP activity in vivo. The tracer uptake was a significantly correlated with regions stained positive for macrophages, MMP-2 and MMP-9 on histology [103]. Enzymatic activity provides a possibility to use functional contrast agents that are only expressed in after enzymatic conversion. These agents are expected to improve the target-to-background ratio. Ronald et al. [104] investigated a functional contrast agent that was expected to oligomerize and bind to resident proteins as a result of myeloperoxidase-mediated activation. It was expected that this would result in a higher magnetic resonance signal and prolonged retention of the contrast agent within myeloperoxidase-rich plaque. The functional contrast agent created focal areas of twofold MRI signal intensity increase in the diseased vessel wall of NZW rabbits, while untargeted contrast agents showed no increase in signal intensity (Fig. 24.9) [104]. Functional contrast agents are an interesting development in in vivo imaging and might result in significant improvements in molecular imaging.

Neovascularization Angiogenesis is seen in numerous malignant, inflammatory, and ischemic diseases. In a healthy person the vascular endothelium is quiescent with less than 0.01% of the endothelial cells undergoing division. This makes angiogenic activity a specific marker for the presence of a disease process. In vascular disease excessive angiogenesis is seen in vascular malformations, hemangioma, hemangioendothelioma, and atherosclerosis [105].

Both MRI and ultrasound can identify the presence of vascularization in an atherosclerotic plaque, using a nontargeted contrast agent. The capability of ultrasound to detect individual microbubbles, which are obligatory intravascular, allows it to detect individual vessels in the plaque [106]. Several studies have shown an association between contrast enhancement in the plaque and intraplaque neovascularization on histology [107–109]. Kerwin et al. investigated dynamic contrast-enhanced MRI measurements of K^{trans} (a contrast transfer constant) and plasma volume in the plaque as measurement of intraplaque neovascularization. A significant correlation was found between dynamic contrast-enhanced MRI measurements and the amount of plaque neovascularization seen on histology [110, 111]. However, both ultrasound and dynamic contrast-enhanced MRI do not show whether there is active angiogenesis in the plaque.

Active angiogenesis can be identified by imaging targets that are overexpressed by proliferating endothelium but not by normal endothelium. The VEGF receptors and the transforming growth factor-β binding receptor endoglin are promising targets which are upregulated in the proliferating endothelium under the influence of HIF-1α [39]. Known for their involvement in tumor angiogenesis both have been targeted in vivo for the detection of tumor angiogenesis in mice using microbubbles or radionuclides [112–115]. The first study using VEGF receptor 2-targeted microbubbles in humans is currently being performed in patients with prostate cancer (clinicaltrials.gov; study no: NCT01253213). Studies investigating the molecular imaging of the VEGF receptors or endoglin have not yet been performed in an atherosclerosis model.

Integrin αvβ3 is a cell surface receptor involved in the migration of endothelial cells across the basement membrane during angiogenesis. Integrin αvβ3 is part of a large family of cell surface receptors, present in both healthy and angiogenic vessels [116]. However, the expression of integrin αvβ3 has been shown to be a marker for angiogenesis present in the adventitial vasa vasorum and intraplaque neovascularization [117–119].

Integrin αvβ3-targeted contrast agents have extensively been investigated in tumor models using MRI [120, 121], PET [122], SPECT [123–125], and ultrasound [114, 126, 127]. In vivo imaging of an atherosclerosis model has only been performed using integrin αvβ3-targeted gadolinium compounds. These compounds were shown to create a significant increase in the MRI signal in the vessel wall at locations of atherosclerosis. The expression of integrin αvβ3, proliferation of angiogenic vessels, and neointima formation was confirmed by histology [120, 121]. However, the results of a clinical trial investigating a ^{99m}Tc-labeled anti-αvβ3 antibody in metastatic cancer patients have thus far been disappointing [128].

During angiogenesis ECM molecules are seen that are not present otherwise. The fibronectin extra-domain B (ED-B) is an isoform of fibronectin, resulting from alternative splicing, which is present in the temporary extracellular matrix formed during tissue remodeling and is hardly present in normal vascular tissue [129]. Increased expression of ED-B has been found in both murine and human plaques. The expression of ED-B in human plaques was predominantly found around the vasa vasorum [130]. Matter et al. developed ^{125}I-labeled monoclonal antibodies against ED-B and found it to specifically target atherosclerotic plaques in apoE knockout mice [130]. However, only ex vivo imaging was performed.

In vivo imaging of the ED-B has been performed in patients with brain, lung, or colorectal cancer. Twenty patients with several different types of malignant tumors received an injection of a ^{123}I-labeled monoclonal antibody against the ED-B (L19). SPECT images were obtained at 4 and 24 h after contrast injection. Sixteen of the patients showed uptake in the tumor or metastasis. Of the four negative tumors one was an astrocytoma that of which it is known that it does not express ED-B. The other three could not be explained. Importantly no adverse events were seen [131]. This study showed that accurate specific targeting of the ED-B is possible. However, the spatial resolution of SPECT will probably not be sufficient to image atherosclerotic targets.

Multitargeted Contrast Agents Recently dual- and triple-targeted contrast agents have emerged in an attempt to improve ligand to target binding. Especially under high shear stress conditions attachment of the contrast agent to the target can be impaired. A number of studies have shown that the use of multitargeted contrast agent significantly improves contrast to target binding [75, 114, 132–134]. The investigated multitargeted contrast agents are of relatively large size (microbubbles and microparticles of iron oxide) and are therefore only targeted at intravascular targets.

Dual combinations of VEGF receptor 2 and $\alpha_v\beta_3$-integrin [114], p-selectin and VCAM-1 [132], and ICAM-1 and sialyl Lewis^x (selectins) [133] have been developed for ultrasound and p-selectin and VCAM-1 for MRI [75]. A triple-targeted microbubble targeting p-selectin, VEGF-receptor2, and $\alpha_v\beta_3$-integrin has been developed for ultrasound [134].

5 Theranostics

Molecular imaging allows the simultaneous detection of therapeutic targets and monitoring of treatment effect, a diagnosis-treatment strategy referred to as *theranostics*. Future theranostic strategies in the field of stabilization of atherosclerotic plaques could be targeted against inflammation and modulation of angiogenesis.

Theranostic Probes The delivery of targeted contrast agents to the atherosclerotic plaque presents clear opportunities for simultaneous drug delivery [135] Nanoparticles and microbubbles can be used for both in vivo diagnostic imaging and therapeutic drug delivery (theranostic probes). By localized delivery of drugs lower dosages of more potent drugs can be used, while reaching higher concentrations at the disease location. Due to decreased concentration at non-diseased sites the adverse effects of the drugs may be reduced. Theranostic agents can also transport drugs that cannot be administered otherwise (lipophilic drugs, proteins, silencing RNAs, DNA, etc). The development of theranostic nanoparticles is rapid and several types of nanoparticles have been developed [136–138].

Winter et al. [139] demonstrated the potential of theranostics in atherosclerosis. They used theranostic nanoparticles to identify the presence of integrin αvβ3 expressing vasa vasorum in the aortas of cholesterol fed rabbits and evaluate the effect of targeted treatment on angiogenesis. The lipid soluble anti-angiogenic agent fumagillin was incorporated in a integrin αvβ3-targeted paramagnetic nanoparticle. They evaluated the presence of integrin αvβ3 expressing vasa vasorum by MRI during treatment and 1-week posttreatment. The expression of integrin αvβ3 significantly decreased in the targeted fumagillin treated group, while the nontargeted fumagillin and no-drug group showed no change [139].

In the field of theranostic probes ultrasound microbubbles have a special interest because they can both deliver drugs and actively stimulate the uptake of the drugs. Microbubbles can be loaded with drugs and destroyed at the location of interest by the application of a high acoustic pressure ultrasound wave (within the limits of standard ultrasound equipment), releasing the drug [140, 141]. Besides the transportation of drugs to the target location this has also been shown to cause sonoporation and induction of endocytosis, which increases the local uptake of the drug (Fig. 24.10) [142–144]. Sonoporation is the creation of transient micropores in the cellular membrane due to the oscillation and implosion of microbubbles in an ultrasound beam, thus temporarily increasing cellular membrane permeability. Ultrasound has been shown to be able to induce the uptake of DNA and RNA molecules giving it an interesting prospective for gene therapy [140, 145, 146].

6 Angiogenesis Modulating Therapy

Anti-angiogenic Treatment Treatment of intraplaque neovascularization has been proposed as a possible method to stabilize the atherosclerotic plaque [147]. Inhibition of intraplaque neovascularization in animals has already shown to reduce the macrophage accumulation and progression of atherosclerosis [148–150]. Several anti-angiogenic agents are available or under evaluation in clinical trials for the treatment of cancer (http://www.cancer.gov/clinicaltrials/).

However, there are potential problems that need to be accounted for in transferring the anti-angiogenic strategy from cancer to atherosclerosis. First and foremost, the goal for the treatment of cancer is destruction of the tumor, while destruction of the vessel wall, atherosclerotic or not, is not necessarily a good idea. Atherosclerosis demands a different strategy to attack the vasculature. Furthermore, inhibition of angiogenesis might aggravate ischemic end-organ damage. Several strategies for inducing angiogenesis are being investigated to restore blood flow to regions affected by ischemia

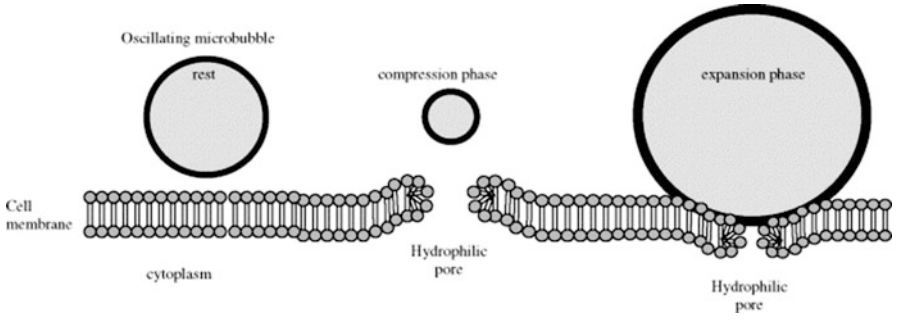

Fig. 24.10 Proposed model of the oscillating microbubble enforced pore formation (sonoporation) in the cell membrane. The pushing and pulling behavior of the microbubble causes rupture of the cell membrane creating a hydrophilic pore allowing trans-membrane flux of fluid and macromolecules. Reproduced with permission from van Wamel et al. [143]

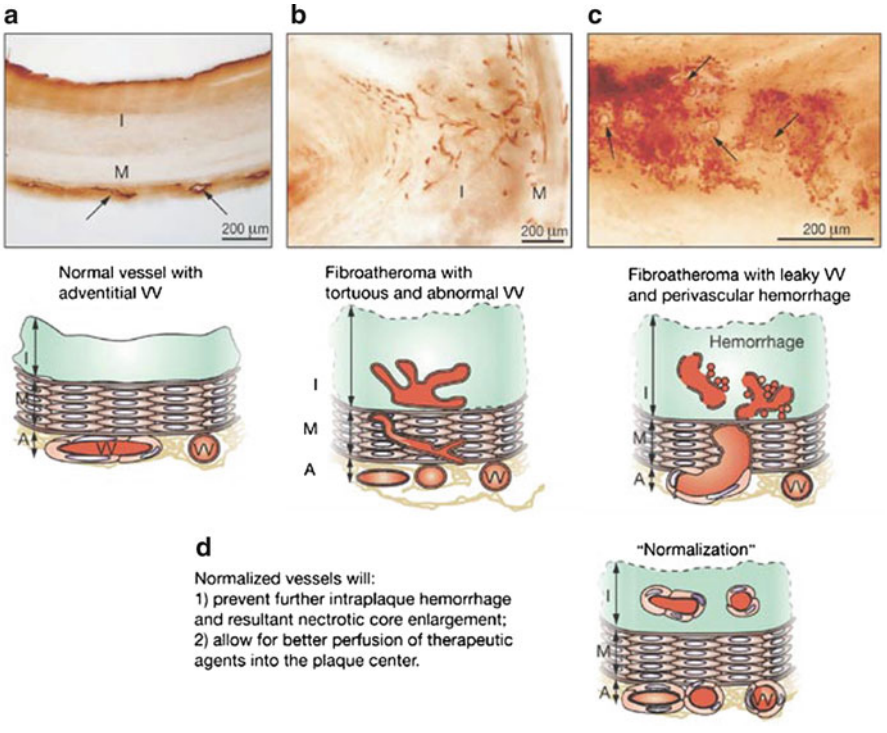

Fig. 24.11 Proposed 'normalization' of plaque microvasculature and its implications in atherosclerotic angiogenesis. Images of 150 m-thick sections of (**a**) normal human coronary artery, and (**b**) fibroatheroma without and (**c**) fibroatheroma with intraplaque hemorrhage. The endothelium was visualized by use of *Ulex europaeus* immunohistochemical staining. (**a**) Adventitial vasa vasorum can be seen (arrows). (**b**) In non-hemorrhagic fibroatheroma the vasa vasorum are intimal and show tortuosity and branching. (**c**) In fibroatheromas with intraplaque hemorrhage the vasa vasorum are disrupted (*arrows*) with surrounding hemorrhage. Intraplaque hemorrhage has been shown to contribute to the necrotic core enlargement and vulnerability to rupture. These specimens (**a**–**c**) are illustrated in corresponding schematics below them. (**d**) Jain et al. hypothesize that normalization of the vasa vasorum with "muscularization" of the capillaries leads to stable vessels that will prevent plaque progression. The absence of leaky vessels should promote plaque stabilization by preventing plaque hemorrhages. *A* adventitia, *I* intima, *M* media, *VV* vasa vasorum. Reproduced with permission from Jain et al. [156]

[151]. This might be overcome by using theranostics to locally deliver antiangiogenic therapy to the plaque.

Destruction of the intraplaque neovasculature could lead to sustained or increased hypoxia. This in turn could lead to further upregulation of genes that promote plaque vulnerability. Rather than eliminating the neovasculature it has been proposed that normalization of the vasculature could help stabilize the plaque [152]. The normalization of the immature intraplaque neovascularization should prevent leakage of erythrocytes, extravasation of lipids, and inflammatory cells that contribute to plaque progression (Fig. 24.11). Furthermore, the presence of these vessels should alleviate hypoxia, thus removing the underlying cause of angiogenesis.

Pro-angiogenic Treatment The induction of angiogenesis by ultrasound contrast agents is currently being explored as a means to restore blood flow in regions affected by ischemia. Targeted stimulation of neovascularization could be of clinical relevance for patients with myocardial ischemia or critical limb ischemia as an alternative treatment strategy for surgical revascularization. Chappell et al. [151] studied microvascular remodeling in a mouse gracilis muscle model. After high-dose administration of microbubble contrast agent and ultrasonic destruction of the microbubbles an impermanent microvascular remodeling response occurred. In contrast to that study, Johnson et al. [152] reported on the bioeffects of microbubble destruction in a gracilis muscle model of 23 Sprague–Dawley rats. Ultrasonic destruction of microbubble contrast agent caused an acute decrease in capillary density, followed by an incomplete angiogenic healing response. In a subsequent study, the gracilis muscles of 150 Sprague–Dawley rats were studied. A statistically significant change in vascular endothelial growth factor (VEGF) was observed, while capillary density was not changed by ultrasonic destruction of microbubble contrast agent [153]. Clearly, further studies are needed to explore the mechanism of action and treatment effect of pro-angiogenic therapy.

7 Conclusions

– Inflammation and angiogenesis are closely related and important factors in early plaque development and plaque vulnerability.

- Molecular imaging can aid in the early detection of plaque formation, provide insights into the natural history of cardiovascular diseases, and function as a surrogate endpoint in clinical trials.
- Several molecular targets involving inflammation and angiogenesis have been identified and tested in vivo; however, the number of contrast agents available for human studies is limited.
- Multimodality imaging and multitargeted contrast agents may improve the accuracy with which a biological process can be identified.
- Future developments in theranostics and antiangiogenic therapy might provide a noninvasive technique for stabilizing the vulnerable plaque.

References

1. Giroud D et al (1992) Relation of the site of acute myocardial infarction to the most severe coronary arterial stenosis at prior angiography. Am J Cardiol 69(8):729–732
2. Pasterkamp G et al (1998) Relation of arterial geometry to luminal narrowing and histologic markers for plaque vulnerability: the remodeling paradox. J Am Coll Cardiol 32(3):655–662
3. Schoenhagen P et al (2000) Extent and direction of arterial remodeling in stable versus unstable coronary syndromes: an intravascular ultrasound study. Circulation 101(6):598–603
4. Hardie AD et al (2007) The impact of expansive arterial remodeling on clinical presentation in carotid artery disease: a multidetector CT angiography study. AJNR Am J Neuroradiol 28(6):1067–1070
5. Naghavi M et al (2003) From vulnerable plaque to vulnerable patient: a call for new definitions and risk assessment strategies: part I. Circulation 108(14):1664–1672
6. Schaar JA et al (2004) Terminology for high-risk and vulnerable coronary artery plaques. Eur Heart J 25(12):1077–1082
7. Virmani R et al (2000) Lessons from sudden coronary death: a comprehensive morphological classification scheme for atherosclerotic lesions. Arterioscler Thromb Vasc Biol 20(5):1262–1275
8. Virmani R et al (2006) Pathology of the vulnerable plaque. J Am Coll Cardiol 47 (8 Suppl):C13–C18
9. Ylä-Herttuala S et al (2011) Stabilisation of atherosclerotic plaques. Thromb Haemost 106(1):1–19
10. Vancraeynest D et al (2011) Imaging the vulnerable plaque. J Am Coll Cardiol 57(20): 1961–1979
11. Cai W et al (2006) How molecular imaging is speeding up antiangiogenic drug development. Mol Cancer Ther 5(11):2624–2633
12. Weissleder R, Pittet MJ (2008) Imaging in the era of molecular oncology. Nature 452(7187):580–589
13. Sanz J, Fayad ZA (2008) Imaging of atherosclerotic cardiovascular disease. Nature 451(7181):953–957
14. Mankoff DA (2007) A definition of molecular imaging. J Nucl Med 48(6):18N–21N
15. Jaffer FA, Weissleder R (2005) Molecular imaging in the clinical arena. JAMA 293(7):855–862
16. Libby P, DiCarli M, Weissleder R (2010) The vascular biology of atherosclerosis and imaging targets. J Nucl Med 51(Suppl 1):33S–37S
17. Maiellaro K, Taylor WR (2007) The role of the adventitia in vascular inflammation. Cardiovasc Res 75(4):640–648
18. Gössl M et al (2010) Segmental heterogeneity of vasa vasorum neovascularization in human coronary atherosclerosis. JACC Cardiovasc Imaging 3(1):32–40
19. Hildebrandt HA et al (2008) Differential distribution of vasa vasorum in different vascular beds in humans. Atherosclerosis 199(1):47–54
20. Wolinsky H, Glagov S (1967) Nature of species differences in the medial distribution of aortic vasa vasorum in mammals. Circ Res 20(4):409–421
21. Heistad DD et al (1981) Role of vasa vasorum in nourishment of the aortic wall. Am J Physiol Heart Circ Physiol 240(5):H781–H787
22. Wilens SL, Malcolm JA, Vasquez JM (1965) Experimental infarction (medial necrosis) of the dog's aorta. Am J Pathol 47(4):695–711
23. Stefanadis C et al (1995) Aorta: structure/function: effect of vasa vasorum flow on structure and function of the aorta in experimental animals. Circulation 91(10):2669–2678
24. Wolinsky H, Glagov S (1969) Comparison of abdominal and thoracic aortic medial structure in mammals. Circ Res 25(6):677–686
25. Gössl M et al (2003) Functional anatomy and hemodynamic characteristics of vasa vasorum in the walls of porcine coronary arteries. Anat Rec A Discov Mol Cell Evol Biol 272(2):526–537
26. Jeziorska M, Woolley DE (1999) Local neovascularization and cellular composition within vulnerable regions of atherosclerotic plaques of human carotid arteries. J Pathol 188(2):189–196
27. Moreno PR et al (2004) Plaque neovascularization is increased in ruptured atherosclerotic lesions of human aorta: implications for plaque vulnerability. Circulation 110(14):2032–2038
28. Mofidi R et al (2001) Association between plaque instability, angiogenesis and symptomatic carotid occlusive disease. Br J Surg 88(7):945–950
29. Purushothaman KR et al (2003) Neovascularization is the most powerful independent predictor for progression to disruption in high-risk atherosclerotic plaques. J Am Coll Cardiol 41(6 Suppl 2):352–353
30. Hellings WE et al (2010) Composition of carotid atherosclerotic plaque is associated with cardiovascular outcome. A prognostic study. Circulation 121(17):1941–1950
31. Mause SF, Weber C (2009) Intrusion through the fragile back door: immature plaque microvessels as entry portals for leukocytes and erythrocytes in atherosclerosis. J Am Coll Cardiol 53(17):1528–1531
32. McCarthy MJ et al (1999) Angiogenesis and the atherosclerotic carotid plaque: an association between symptomatology and plaque morphology. J Vasc Surg 30(2):261–268
33. Dunmore BJ et al (2007) Carotid plaque instability and ischemic symptoms are linked to immaturity of microvessels within plaques. J Vasc Surg 45(1):155–159
34. Sluimer J et al (2009) Thin-walled microvessels in human coronary atherosclerotic plaques show incomplete endothelial junctions relevance of compromised structural integrity for intraplaque microvascular leakage. J Am Coll Cardiol 53(17):1517–1527
35. Sluimer JC, Daemen MJ (2009) Novel concepts in atherogenesis: angiogenesis and hypoxia in atherosclerosis. J Pathol 218(1):7–29
36. Kolodgie FD et al (2003) Intraplaque hemorrhage and progression of coronary atheroma. N Engl J Med 349(24):2316–2325
37. Moulton KS (2006) Angiogenesis in atherosclerosis: gathering evidence beyond speculation. Curr Opin Lipidol 17(5):548–555
38. Carmeliet P (2000) Mechanisms of angiogenesis and arteriogenesis. Nat Med 6(4):389–395

39. Semenza GL (2003) Targeting HIF-1 for cancer therapy. Nat Rev Cancer 3(10):721–732
40. Pugh CW, Ratcliffe PJ (2003) Regulation of angiogenesis by hypoxia: role of the HIF system. Nat Med 9(6):677–684
41. Sluimer JC et al (2008) Hypoxia, hypoxia-inducible transcription factor, and macrophages in human atherosclerotic plaques are correlated with intraplaque angiogenesis. J Am Coll Cardiol 51(13):1258–1265
42. Bjornheden T et al (1999) Evidence of hypoxic areas within the arterial wall in vivo. Arterioscler Thromb Vasc Biol 19(4):870–876
43. Jeziorska M, Woolley DE (1999) Neovascularization in early atherosclerotic lesions of human carotid arteries: its potential contribution to plaque development. Hum Pathol 30(8):919–925
44. Fleiner M et al (2004) Arterial neovascularization and inflammation in vulnerable patients: early and late signs of symptomatic atherosclerosis. Circulation 110(18):2843–2850
45. Kwon HM et al (1998) Enhanced coronary vasa vasorum neovascularization in experimental hypercholesterolemia. J Clin Invest 101(8):1551–1556
46. Herrmann J et al (2001) Coronary vasa vasorum neovascularization precedes epicardial endothelial dysfunction in experimental hypercholesterolemia. Cardiovasc Res 51(4):762–766
47. Lusis AJ (2000) Atherosclerosis. Nature 407(6801):233–241
48. Gössl M et al (2009) Low vasa vasorum densities correlate with inflammation and subintimal thickening: potential role in location – determination of atherogenesis. Atherosclerosis 206(2):362–368
49. Bayer I et al (2002) Experimental angiogenesis of arterial vasa vasorum. Cell Tissue Res 307(3):303–313
50. Dobrucki LW, Sinusas AJ (2010) PET and SPECT in cardiovascular molecular imaging. Nat Rev Cardiol 7(1):38–47
51. Sosnovik D, Nahrendorf M, Weissleder R (2008) Magnetic nanoparticles for MR imaging: agents, techniques and cardiovascular applications. Basic Res Cardiol 103(2):122–130
52. Kuo PH et al (2007) Gadolinium-based MR contrast agents and nephrogenic systemic fibrosis. Radiology 242(3):647–649
53. Powers J, Averkiou M, Bruce M (2009) Principles of cerebral ultrasound contrast imaging. Cerebrovasc Dis 27(Suppl 2):14–24
54. Main M, Goldman J, Grayburn P (2009) Ultrasound contrast agents: balancing safety versus efficacy. Expert Opin Drug Saf 8(1):49–56
55. Main ML, Goldman JH, Grayburn PA (2007) Thinking outside the "box" – the ultrasound contrast controversy. J Am Coll Cardiol 50(25):2434–2437
56. Hyafil F et al (2007) Noninvasive detection of macrophages using a nanoparticulate contrast agent for computed tomography. Nat Med 13(5):636–641
57. Cormode DP et al (2008) Nanocrystal core high-density lipoproteins: a multimodality contrast agent platform. Nano Lett 8(11):3715–3723
58. Cormode DP et al (2010) Atherosclerotic plaque composition: analysis with multicolor CT and targeted gold nanoparticles. Radiology 256(3):774–782
59. Rabin O et al (2006) An X-ray computed tomography imaging agent based on long-circulating bismuth sulphide nanoparticles. Nat Mater 5(2):118–122
60. Pontone G et al (2009) Diagnostic accuracy of coronary computed tomography angiography: a comparison between prospective and retrospective electrocardiogram triggering. J Am Coll Cardiol 54(4):346–355
61. Nash K, Hafeez A, Hou S (2002) Hospital-acquired renal insufficiency. Am J Kidney Dis 39(5):930–936
62. Gaemperli O, Kaufmann PA (2011) PET and PET/CT in cardiovascular disease. Ann N Y Acad Sci 1228(1):109–136
63. Izquierdo-Garcia D et al (2009) Comparison of methods for magnetic resonance-guided [18-F]fluorodeoxyglucose positron emission tomography in human carotid arteries: reproducibility, partial volume correction, and correlation between methods. Stroke 40(1):86–93
64. Mulder WJ et al (2007) Magnetic and fluorescent nanoparticles for multimodality imaging. Nanomedicine 2(3):307–324
65. Nahrendorf M et al (2008) Nanoparticle PET-CT imaging of macrophages in inflammatory atherosclerosis. Circulation 117(3):379–387
66. O'Brien KD et al (1993) Vascular cell adhesion molecule-1 is expressed in human coronary atherosclerotic plaques. Implications for the mode of progression of advanced coronary atherosclerosis. J Clin Invest 92(2):945–951
67. O'Brien KD et al (1996) Neovascular expression of e-selectin, intercellular adhesion molecule-1, and vascular cell adhesion molecule-1 in human atherosclerosis and their relation to intimal leukocyte content. Circulation 93(4):672–682
68. Kelly KA et al (2005) Detection of vascular adhesion molecule-1 expression using a novel multimodal nanoparticle. Circ Res 96(3):327–336
69. Nahrendorf M et al (2006) Noninvasive vascular cell adhesion molecule-1 imaging identifies inflammatory activation of cells in atherosclerosis. Circulation 114(14):1504–1511
70. Kaufmann BA et al (2007) Molecular imaging of inflammation in atherosclerosis with targeted ultrasound detection of vascular cell adhesion molecule-1. Circulation 116(3):276–284
71. Villanueva FS et al (1998) Microbubbles targeted to intercellular adhesion molecule-1 bind to activated coronary artery endothelial cells. Circulation 98(1):1–5
72. Demos SM et al (1999) In vivo targeting of acoustically reflective liposomes for intravascular and transvascular ultrasonic enhancement. J Am Coll Cardiol 33(3):867–875
73. Kang HW et al (2002) Magnetic resonance imaging of inducible e-selectin expression in human endothelial cell culture. Bioconjug Chem 13(1):122–127
74. Kang HW et al (2006) Targeted imaging of human endothelial-specific marker in a model of adoptive cell transfer. Lab Invest 86(6):599–609
75. McAteer MA et al (2008) Magnetic resonance imaging of endothelial adhesion molecules in mouse atherosclerosis using dual-targeted microparticles of iron oxide. Arterioscler Thromb Vasc Biol 28(1):77–83
76. Boutry S et al (2005) Magnetic resonance imaging of inflammation with a specific selectin-targeted contrast agent. Magn Reson Med 53(4):800–807
77. Radermacher KA et al (2009) In vivo detection of inflammation using pegylated iron oxide particles targeted at e-selectin: a multimodal approach using MR imaging and EPR spectroscopy. Invest Radiol 44(7):398–404
78. Moore KJ, Kathryn J, Tabas I (2011) Macrophages in the pathogenesis of atherosclerosis. Cell 145(3):341–355
79. de Boer OJ et al (1999) Leucocyte recruitment in rupture prone regions of lipid-rich plaques: a prominent role for neovascularization? Cardiovasc Res 41(2):443–449
80. Rogers WJ, Basu P (2005) Factors regulating macrophage endocytosis of nanoparticles: implications for targeted magnetic resonance plaque imaging. Atherosclerosis 178(1):67–73
81. Lipinski MJ et al (2006) MRI to detect atherosclerosis with gadolinium-containing immunomicelles targeting the macrophage scavenger receptor. Magn Reson Med 56(3):601–610
82. Schmitz SA et al (2001) Magnetic resonance imaging of atherosclerotic plaques using superparamagnetic iron oxide particles. J Magn Reson Imaging 14(4):355–361

83. Kooi ME et al (2003) Accumulation of ultrasmall superparamagnetic particles of iron oxide in human atherosclerotic plaques can be detected by in vivo magnetic resonance imaging. Circulation 107(19):2453–2458
84. Trivedi RA et al (2004) In vivo detection of macrophages in human carotid atheroma: temporal dependence of ultrasmall superparamagnetic particles of iron oxide-enhanced MRI. Stroke 35(7):1631–1635
85. Trivedi RA et al (2006) Identifying inflamed carotid plaques using in vivo USPIO-enhanced MR imaging to label plaque macrophages. Arterioscler Thromb Vasc Biol 26(7):1601–1606
86. Kawahara I et al (2008) Potential of magnetic resonance plaque imaging using superparamagnetic particles of iron oxide for the detection of carotid plaque. Neurol Med Chir (Tokyo) 48(4):157–161
87. Tang TY et al (2009) The ATHEROMA (Atorvastatin Therapy: Effects on Reduction of Macrophage Activity) study: evaluation using ultrasmall superparamagnetic iron oxide-enhanced magnetic resonance imaging in carotid disease. J Am Coll Cardiol 53(22):2039–2050
88. Yun M et al (2001) F-18 FDG uptake in the large arteries: a new observation. Clin Nucl Med 26(4):314–319
89. Lederman RJ et al (2001) Detection of atherosclerosis using a novel positron-sensitive probe and 18-fluorodeoxyglucose (FDG). Nucl Med Commun 22(7):747–753
90. Ogawa M et al (2004) (18)F-FDG accumulation in atherosclerotic plaques: immunohistochemical and PET imaging study. J Nucl Med 45(7):1245–1250
91. Tawakol A et al (2005) Noninvasive in vivo measurement of vascular inflammation with F-18 fluorodeoxyglucose positron emission tomography. J Nucl Cardiol 12(3):294–301
92. Ogawa M et al (2006) Application of 18F-FDG PET for monitoring the therapeutic effect of antiinflammatory drugs on stabilization of vulnerable atherosclerotic plaques. J Nucl Med 47(11):1845–1850
93. Rudd JHF et al (2002) Imaging atherosclerotic plaque inflammation with [18F]-fluorodeoxyglucose positron emission tomography. Circulation 105(23):2708–2711
94. Tawakol A et al (2006) In vivo 18F-fluorodeoxyglucose positron emission tomography imaging provides a noninvasive measure of carotid plaque inflammation in patients. J Am Coll Cardiol 48(9):1818–1824
95. Tahara N et al (2007) Vascular inflammation evaluated by [18F]-fluorodeoxyglucose positron emission tomography is associated with the metabolic syndrome. J Am Coll Cardiol 49(14):1533–1539
96. Tahara N et al (2007) The prevalence of inflammation in carotid atherosclerosis: analysis with fluorodeoxyglucose positron emission tomography. Eur Heart J 28(18):2243–2248
97. Rudd JHF et al (2008) Atherosclerosis inflammation imaging with 18F-FDG PET: carotid, iliac, and femoral uptake reproducibility, quantification methods, and recommendations. J Nucl Med 49(6):871–878
98. Davies JR et al (2005) Identification of culprit lesions after transient ischemic attack by combined 18F fluorodeoxyglucose positron-emission tomography and high-resolution magnetic resonance imaging. Stroke 36(12):2642–2647
99. Rominger A et al (2009) 18F-FDG PET/CT identifies patients at risk for future vascular events in an otherwise asymptomatic cohort with neoplastic disease. J Nucl Med 50(10):1611–1620
100. Tahara N et al (2006) Simvastatin attenuates plaque inflammation: evaluation by fluorodeoxyglucose positron emission tomography. J Am Coll Cardiol 48(9):1825–1831
101. Galis ZS, Khatri JJ (2002) Matrix metalloproteinases in vascular remodeling and atherogenesis: the good, the bad, and the ugly. Circ Res 90(3):251–262
102. Lancelot E et al (2008) Evaluation of matrix metalloproteinases in atherosclerosis using a novel noninvasive imaging approach. Arterioscler Thromb Vasc Biol 28(3):425–432
103. Ohshima S et al (2009) Molecular imaging of matrix metalloproteinase expression in atherosclerotic plaques of mice deficient in apolipoprotein E or low-density-lipoprotein receptor. J Nucl Med 50(4):612–617
104. Ronald JA et al (2009) Enzyme-sensitive magnetic resonance imaging targeting myeloperoxidase identifies active inflammation in experimental rabbit atherosclerotic plaques. Circulation 120(7):592–599
105. Carmeliet P, Jain RK (2000) Angiogenesis in cancer and other diseases. Nature 407(6801): 249–257
106. Staub D et al (2010) Contrast-enhanced ultrasound imaging of the vasa vasorum: from early atherosclerosis to the identification of unstable plaques. JACC Cardiovasc Imaging 3(7):761–771
107. Shah F et al (2007) Contrast-enhanced ultrasound imaging of atherosclerotic carotid plaque neovascularization: a new surrogate marker of atherosclerosis? Vasc Med 12(4):291–297
108. Coli S et al (2008) Contrast-enhanced ultrasound imaging of intraplaque neovascularization in carotid arteries: correlation with histology and plaque echogenicity. J Am Coll Cardiol 52(3):223–230
109. Giannoni MF et al (2009) Contrast carotid ultrasound for the detection of unstable plaques with neoangiogenesis: a pilot study. Eur J Vasc Endovasc Surg 37(6):722–727
110. Kerwin W et al (2003) Quantitative magnetic resonance imaging analysis of neovasculature volume in carotid atherosclerotic plaque. Circulation 107(6):851–856
111. Kerwin WS et al (2008) MR imaging of adventitial vasa vasorum in carotid atherosclerosis. Magn Reson Med 59(3):507–514
112. Bredow S et al (2000) Imaging of tumour neovasculature by targeting the TGF-[beta] binding receptor endoglin. Eur J Cancer 36(5):675–681
113. Korpanty G et al (2007) Monitoring response to anticancer therapy by targeting microbubbles to tumor vasculature. Clin Cancer Res 13(1):323–330
114. Willmann J et al (2008) Dual-targeted contrast agent for US assessment of tumor angiogenesis in vivo. Radiology 248(3):936–944
115. Pochon SP et al (2010) BR55: a lipopeptide-based VEGFR2-targeted ultrasound contrast agent for molecular imaging of angiogenesis. Invest Radiol 45(2):89–95
116. Hynes RO (1987) Integrins: a family of cell surface receptors. Cell 48(4):549–554
117. Hoshiga M et al (1995) Alpha-v beta-3 integrin expression in normal and atherosclerotic artery. Circ Res 77(6):1129–1135
118. Brooks PC, Clark RA, Cheresh DA (1994) Requirement of vascular integrin alpha v beta 3 for angiogenesis. Science 264(5158):569–571
119. Haubner R (2006) Alpha v beta 3-integrin imaging: a new approach to characterise angiogenesis? Eur J Nucl Med Mol Imaging 33(Suppl 1):54–63
120. Winter PM et al (2003) Molecular imaging of angiogenesis in early-stage atherosclerosis with alpha(v)beta3-integrin-targeted nanoparticles. Circulation 108(18):2270–2274
121. Burtea C et al (2008) Molecular imaging of alpha v beta 3 integrin expression in atherosclerotic plaques with a mimetic of RGD peptide grafted to Gd-DTPA. Cardiovasc Res 78(1):148–157
122. Haubner R et al (2005) Noninvasive visualization of the activated alphavbeta3 integrin in cancer patients by positron emission tomography and [18F] Galacto-RGD. PLoS Med 2(3):e70
123. Meoli D et al (2004) Noninvasive imaging of myocardial angiogenesis following experimental myocardial infarction. J Clin Invest 113(12):1684–1691

124. Sadeghi MM et al (2004) Detection of injury-induced vascular remodeling by targeting activated {alpha}v{beta}3 integrin in vivo. Circulation 110(1):84–90
125. Hua J et al (2005) Noninvasive imaging of angiogenesis with a 99mTc-labeled peptide targeted at [alpha]v[beta]3 integrin after murine hindlimb ischemia. Circulation 111(24):3255–3260
126. Ellegala DB et al (2003) Imaging tumor angiogenesis with contrast ultrasound and microbubbles targeted to [alpha]v[beta]3. Circulation 108(3):336–341
127. Leong-Poi H et al (2003) Noninvasive assessment of angiogenesis by ultrasound and microbubbles targeted to alpha(v)-integrins. Circulation 107(3):455–460
128. Posey JA et al (2001) A pilot trial of vitaxin, a humanized anti-vitronectin receptor (anti αvβ3) antibody in patients with metastatic cancer. Cancer Biother Radiopharm 16(2):125–132
129. Castellani P et al (2002) Differentiation between high-and low-grade astrocytoma using a human recombinant antibody to the extra domain-B of fibronectin. Am J Pathol 161(5):1695–1700
130. Matter CM et al (2004) Molecular imaging of atherosclerotic plaques using a human antibody against the extra-domain B of fibronectin. Circ Res 95(12):1225–1233
131. Santimaria M et al (2003) Immunoscintigraphic detection of the ED-B domain of fibronectin, a marker of angiogenesis, in patients with cancer. Clin Cancer Res 9(2):571–579
132. Ferrante EA et al (2009) Dual targeting improves microbubble contrast agent adhesion to VCAM-1 and P-selectin under flow. J Control Release 140(2):100–107
133. Weller GER et al (2005) Targeted ultrasound contrast agents: in vitro assessment of endothelial dysfunction and multi-targeting to ICAM-1 and sialyl Lewisx. Biotechnol Bioeng 92(6):780–788
134. Warram JM et al (2011) A triple-targeted ultrasound contrast agent provides improved localization to tumor vasculature. J Ultrasound Med 30(7):921–931
135. Lee DY, Li KCP (2011) Molecular theranostics: a primer for the imaging professional. AJR Am J Roentgenol 197(2):318–324
136. Wickline SA et al (2006) Applications of nanotechnology to atherosclerosis, thrombosis, and vascular biology. Arterioscler Thromb Vasc Biol 26(3):435–441
137. Sahoo SK, Labhasetwar V (2003) Nanotech approaches to drug delivery and imaging. Drug Discov Today 8(24):1112–1120
138. Sandhiya S, Dkhar SA, Surendiran A (2009) Emerging trends of nanomedicine – an overview. Fundam Clin Pharmacol 23(3):263–269
139. Winter PM et al (2006) Endothelial alpha(v)beta3 integrin-targeted fumagillin nanoparticles inhibit angiogenesis in atherosclerosis. Arterioscler Thromb Vasc Biol 26(9):2103–2109
140. Newman CMH, Bettinger T (2007) Gene therapy progress and prospects: ultrasound for gene transfer. Gene Ther 14(6):465–475
141. Frinking PJA et al (1998) Effect of ultrasound on the release of micro-encapsulated drugs. Ultrasonics 36(1–5):709–712
142. Ohl CD et al (2006) Sonoporation from jetting cavitation bubbles. Biophys J 91(11): 4285–4295
143. van Wamel A et al (2006) Vibrating microbubbles poking individual cells: drug transfer into cells via sonoporation. J Control Release 112(2):149–155
144. Meijering BDM et al (2009) Ultrasound and microbubble-targeted delivery of macromolecules is regulated by induction of endocytosis and pore formation. Circ Res 104(5):679–687
145. Kobulnik J et al (2009) Comparison of gene delivery techniques for therapeutic angiogenesis: ultrasound-mediated destruction of carrier microbubbles versus direct intramuscular injection. J Am Coll Cardiol 54(18):1735–1742
146. Suzuki JI et al (2010) Ultrasound-microbubble-mediated intercellular adhesion molecule-1 small interfering ribonucleic acid transfection attenuates neointimal formation after arterial injury in mice. J Am Coll Cardiol 55(9):904–913
147. Finn AV, Jain RK (2010) Coronary plaque neovascularization and hemorrhage: a potential target for plaque stabilization? JACC Cardiovasc Imaging 3(1):41–44
148. Moulton KS et al (2003) Inhibition of plaque neovascularization reduces macrophage accumulation and progression of advanced atherosclerosis. Proc Natl Acad Sci USA 100(8):4736–4741
149. Gössl M et al (2009) Prevention of vasa vasorum neovascularization attenuates early neointima formation in experimental hypercholesterolemia. Basic Res Cardiol 104(6):695–706
150. Moulton KS et al (1999) Angiogenesis inhibitors endostatin or TNP-470 reduce intimal neovascularization and plaque growth in apolipoprotein E-deficient mice. Circulation 99(13):1726–1732
151. Chappell JC, Klibanov AL, Price RJ (2005) Ultrasound-microbubble-induced neovascularization in mouse skeletal muscle. Ultrasound Med Biol 31(10):1411–1422
152. Johnson CA, Sarwate S, Miller RJ, O'Brien WD (2010) A temporal study of ultrasound contrast agent-induced changes in capillary density. J Ultrasound Med 29(9):1267–1275
153. Johnson CA, Miller RJ, O'Brien WD (2011) Ultrasound contrast agents affect the angiogenic response. J Ultrasound Med 30(7):933–941
154. ten Kate GL et al (2010) Molecular imaging of inflammation and intraplaque vasa vasorum: a step forward to identification of vulnerable plaques? J Nucl Cardiol 17(5):897–912
155. Sipkins DA et al (2000) ICAM-1 expression in autoimmune encephalitis visualized using magnetic resonance imaging. J Neuroimmunol 104(1):1–9
156. Jain RK et al (2007) Antiangiogenic therapy for normalization of atherosclerotic plaque vasculature: a potential strategy for plaque stabilization. Nat Clin Pract Cardiovasc Med 4(9):491–502
157. Schoenenberger F, Mueller A (1960) Ueber die vaskularisierung der rinderaortenwand. Helvet Physiol Pharmacol Acta 18:136–150